

---

**CHAPTER-3**

**EXPERIMENTAL METHODS**

---

## CHAPTER 3

### EXPERIMENTAL METHODS

#### 3.1: The Site

The present study was carried out at Tezpur University campus location (26°37' N and 92°50' E, elevated about 48 m above mean sea level) on the north bank of Brahmaputra river (Fig.3.1) under the MAPAN (Monitoring of Atmospheric Pollution and Networking) programme of IITM-Pune (an institute under the sponsorship of Ministry of Earth Science, Government of India). The site may be specified as a rural residential/institutional area. Tezpur city is lightly populated and the moderately busy highways are located at about 20 km from the study site. The eastern Himalayan ranges begin at a distance of 40 km on the north. The region is still developing. Traditional biomass burning in homes, agriculture, lush green vegetation and forest are seen in the surrounding areas of the study site as previously reported [1]. The city Tezpur is the largest city in North bank towns and has a population of about 2.0 million with a population density of 365 per square km [2]. Tezpur is the Administrative Headquarter of Sonitpur district in Assam, India. The State of Assam has over 1.8 million registered vehicles for transport and non-transport purposes as on 31st March 2012.

The climate in Tezpur is warm and temperate. When compared with winter, the summers have much more rainfall. The average temperature in Tezpur is 24.4 °C. The average annual rainfall is 1836 mm. Tezpur experiences four distinct seasons: pre-monsoon (march–may), monsoon (June–September), post-monsoon (October–December), and winter (January–February). Frequent inversion and calm conditions prevail during the winter. Excessive humidity is observed in the area. Wind pattern observed were mostly northerly and north easterly with mostly calm condition during monsoon season except the Bordoisila (a feral type of wind that signs the advent of monsoon) [3].

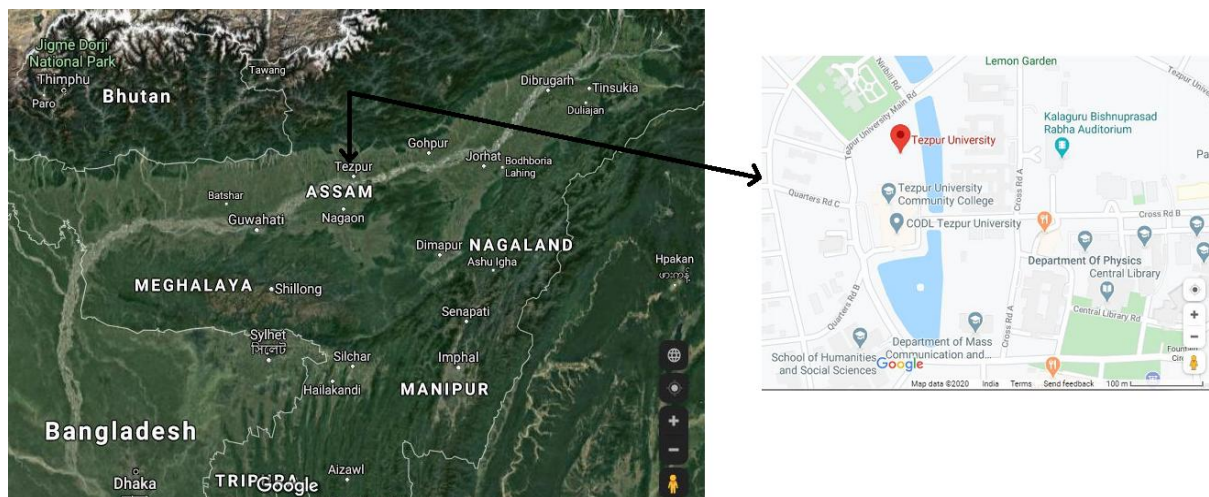


Fig 3.1: (A) Map showing Tezpur and the Brahmaputra Valley region along with the neighboring regions (B) Map of Tezpur University study site (Image Courtesy: Google maps)

### **3.2: Measurement Techniques**

Continuous measurements of ambient ozone ( $O_3$ ) and its precursors Oxides of Nitrogen ( $NO_x$ ), Carbon monoxide (CO) and Total non-methane hydrocarbon (TNMHC) along with meteorological parameters were monitored for a period of four years i.e from May 2013 to December 2017 in order to investigate the relationship of ozone with its precursor compounds and also to understand how meteorological conditions affect the ozone formation and its relationships with precursors. The data was obtained from an automated instrument known as Combined Ambient Air Quality Monitoring Station (CAAQMS) installed in the Department of Environmental Science, Tezpur University under the MAPAN (Monitoring of atmospheric pollution and Networking) project in collaboration with Indian Institute of Tropical Meteorology (IITM), Pune and Ministry of Earth Sciences (MOES) and Government of India (GOI). The Meteorological parameters were also recorded simultaneously with a mechanized weather tracking system installed as a part of CAAQMS. The data obtained from the instrument were in raw format which were then processed in IITM, Pune. The data of all parameters were logged at a 5 min interval and then averaged to hourly values. These hourly values were then used for the study.

### **3.2.1: Ozone (O<sub>3</sub>)**

Ambient O<sub>3</sub> concentrations were measured using a Serinus 10 ozone analyzer. This analyzer uses non-dispersive ultraviolet (UV) absorption technology to measure ozone to a sensitivity of 0.5 ppb in the range of 0-20 ppm.

The analyzer measures ozone with the following components:-

- Mercury vapour lamp
- Photodiode detector
- Ozone scrubber

The concentration of O<sub>3</sub> is automatically corrected for gas temperature and pressure changes and referred to 0°C, 20°C, or 25°C at 1 atmosphere.

#### **Measurement Theory:**

The measurement of ambient O<sub>3</sub> is determined by UV absorption analysis. The UV photometer determines the concentration of ozone in a sample gas at ambient pressure by detecting the absorption of UV radiation in a glass absorption tube. Ozone shows strong absorption of UV light at 254 nm. Sample air is passed into the glass absorption tube (measurement cell). Within this cell a single beam of UV radiation passes through the sample and is absorbed by the O<sub>3</sub>. The solar blind vacuum photodiode detects any UV that is not absorbed. The strength of the UV signal being detected is proportional to the amount of UV light being absorbed by O<sub>3</sub>. The Serinus 10 analyzer uses Beer-Lambert relationship to calculate the concentrations of O<sub>3</sub>. Ozone is not only the gas that absorbs UV (254nm), SO<sub>2</sub> and aromatic compounds also absorb radiation at this wavelength. To eliminate this interference a second cycle is performed where sample air is passed through an O<sub>3</sub> scrubber which allows all interfering gases through but eliminates O<sub>3</sub> thereby accurately measuring interfering gases effects on signal and removing them from the sample measurement signal [4].

### **3.2.2: Oxides of Nitrogen (NO<sub>x</sub>)**

Continuous measurement of oxides of Nitrogen (NO<sub>x</sub>) were carried out using a Serinus 40 Oxides of Nitrogen analyzer that uses gas phase chemilluminescence detection to perform continuous analysis of Nitric Oxide (NO), total oxides of nitrogen (NO<sub>x</sub>), and

Nitrogen dioxide (NO<sub>2</sub>). The serinus 40 analyzer measures to a sensitivity of 0.4 ppb in the range of 0-20 ppm. The measurements of these three gases were performed with the following main sub-components:-

- NO<sub>2</sub> to NO converter
- Delay coil (NO<sub>x</sub> channel)
- Ozone source with reaction chamber
- Photomultiplier tube
- Calculation of NO<sub>2</sub> from NO/NO<sub>x</sub>

The concentrations were automatically corrected for gas temperature and pressure changes and referenced to 0°C, 20°C, or 25°C at 1 atmosphere [5].

SPSS and Excel are used for plotting the concentrations of O<sub>3</sub> and NO<sub>x</sub> as well as their relationships with meteorological parameters and also the different seasonal and monthly trends. The R package, Openair [6-7] was used for analyses and illustrations and in computing the calendar plots, time variation plots and polar plots.

### **3.2.3: Sampling of pollutant during Diwali festival**

The data of ambient O<sub>3</sub>, NO<sub>x</sub>, TNMHC and CO for the study was obtained from the Combined Ambient Air Quality Monitoring Station (CAAQMS) station under the MAPAN project at Tezpur University for the period of four years (15 May 2013-15 May 2017). The data for this study was collected during the Diwali period of these four years. The data was collected for five days i.e. a day of one week before Diwali, a day before Diwali, Diwali day, a day following Diwali and a day of one week after Diwali. The diel patterns of ambient O<sub>3</sub> and its precursors during the Diwali days were observed by using this data.

### **3.2.4: Sampling of pollutant during solar eclipse hours**

The data of ambient O<sub>3</sub>, NO<sub>x</sub>, NO and NO<sub>2</sub> along with meteorological parameters for the study was obtained from the Combined Ambient Air Quality Monitoring Station (CAAQMS) station under the MAPAN project at Tezpur University during solar eclipse hours as well as normal days for the year 2014 and 2015. The data was collected for five days i.e. two days prior solar eclipse event, a day before the eclipse hours, eclipse day, a

day following eclipse day and a day after that. The diel patterns of ambient O<sub>3</sub> and its precursors along with Meteorological parameters during the eclipse hours as well as the normal days were observed by using this data.

### **Description of the solar eclipse on April 29, 2014 and March 20, 2015**

The solar eclipse that occurred on 29<sup>th</sup> April, 2014 was an annular solar eclipse. Annular solar eclipse generally occurs when the surface diameter of the moon is smaller than the sun due to which the moon blocks maximum sunlight making it look like an annulus. The magnitude of the eclipse was 0.9868. Partial eclipse was visible in regions of South India, Australia and Antarctica and annular eclipse was visible in regions of Antarctica. The solar eclipse was visible in Tezpur, India at 11.44 am when the eclipse was at its maximum peak. The eclipse partially began at 3:52 UTC, the total begin time of the eclipse was at 5:47 UTC, greatest eclipse was at 6:04 UTC, total end time of the eclipse was at 6:09 UTC and partial end time was at 8:14 UTC.

The solar eclipse that occurred on 20<sup>th</sup> March, 2015 was a total solar eclipse. Total solar eclipse generally occurs when the surface diameter of the moon is larger than the Sun due to which the direct sunlight of the Sun is blocked turning daylight into darkness. The total solar eclipse was visible in the Faroe Islands and Svalbard and it then passes to North Atlantic and the Arctic Ocean. The magnitude of the eclipse was 1.0445 and the duration was 167 second. The greatest eclipse was at 9:46 UTC. The solar eclipse was visible in Tezpur, India at 9:45 UTC when the eclipse was at its maximum peak. The eclipse was extra special because it occurred on March equinox. The maximum width of the band was 463 km. The eclipse partially began at 7:40 UTC, the total begin time of the eclipse was at 9:09 UTC, greatest eclipse was at 9:45 UTC, total end time of the eclipse was at 10:21 UTC and partial end time was at 11:50 UTC.

### **3.3: Meteorological parameters**

Continuous measurements of meteorological parameters which included relative humidity, solar radiation, temperature, wind speed, wind direction and rainfall were monitored simultaneously with an automated weather tracking system which is installed as a part of the Combined Ambient Air Quality Monitoring Station (CAAQMS) under the MAPAN project installed in the Department of Environmental Science, Tezpur University. The data was recorded from 15 May 2013 and continued till 31<sup>st</sup> December

2017. The gbl files used for calculating back trajectories in PSCF and CWT analyses were obtained from NCEP/NCAR Reanalysis database available at <ftp://arlftp.arlhq.noaa.gov/pub/archives/reanalysis>. Back trajectories were computed using NOAA HYSPLIT model. Reanalysis data were downloaded from gridded meteorological data archives.

The four seasons considered in the study were as per the India Meteorological Department [8]: pre-monsoon (March–May), monsoon (June–September), post-monsoon (October–December), and winter (January–February).

### **3.4: Locating local sources**

#### **Calculation of Conditional probability function and pollution roses**

The direction of ambient O<sub>3</sub> local sources in Tezpur was computed by using pollution roses and Conditional probability function (CPF) in an hourly interval time. Pollution rose is useful for considering pollutant concentrations by wind direction. The probabilities of a particular pollution level in concurrence with definite wind direction were represented graphically and statistically by using pollution roses [9-10]. The wind directions were divided into four parts and thus the pollution roses are given by the following equation:

$$CPF_i = m_i/n_i \quad (3.1)$$

Where,  $m_i$  is the number of probabilities of hourly O<sub>3</sub> concentrations during the occurrence of wind incidents and  $n_i$  is the total number of data occurring at an hourly interval taken from the same set of wind data [11-13]. The CPF criterion threshold for hourly interval O<sub>3</sub> concentrations was set at 75<sup>th</sup> percentile level. CPF clearly identifies the sources which are close to the receptor site [14], thereby identifying the high concentration of air pollution in that region [15].

However, in case of the conditional bivariate probability function (CBPF), wind speed is used as a third variable which pairs with the CPF function thereby assigning both wind speed and wind direction as the pollution concentration indicator of that particular place. The CBPF function is mathematically defined as:

$$CBPF_{\Delta\theta, \Delta u} = m_{\Delta\theta, \Delta u | C \geq x} / n_{\Delta\theta, \Delta u} \quad (3.2)$$

Where,  $m_{\Delta\theta, \Delta u}$  is the wind sector sample number,  $\Delta\theta$  is the interval of the wind speed,  $\Delta u$  is the concentration  $C$  which is greater than  $X$  which is a threshold value and  $n_{\Delta\theta, \Delta u}$  is the wind

direction-speed interval sample number .The introduction of the third variable in CBPF furnishes more detailed information of the source regions than the CPF function and also shows the dependencies of wind speed on the pollution concentrations [15].

### **3.5: Appreciating long range transport and locating source region**

#### **(A) Calculation of backward trajectories and cluster analysis**

The course and origin of the pollutant air masses transported over to the study area were detected by computing backward trajectories at 500 m above ground level by using the TrajStat software which uses NOAA HYSPLIT model to calculate back trajectories. The back trajectories were calculated for 72 hours ensuing every hour between 00:00 hr and 23:00 hr UTC during January 2014 to December 2017 by using the NCEP/NCAR Reanalysis database accessible at <ftp://arlftp.arlhq.noaa.gov/pub/archives/reanalysis> [16]. Trajectory clusters were formed by merging the nearest trajectories using Ward's hierarchical method in Trajstat software. The angular distance was chosen while the cluster number and the cluster model were marked by ocular survey [17]. Trajectories were merged using meteoinfo software.

#### **(B) Potential source contribution function (PSCF)**

PSCF calculations are done to analyze the regional contributions of ambient  $O_3$  in Tezpur. For this study, the study area ( $26.70^\circ$  N and  $92.83^\circ$ E) at 500 m above ground level (AGL) was divided into an array of grid cells of size  $0.5^\circ \times 0.5^\circ$  and then by calculating the trajectory endpoints in each cell, the PSCF values were estimated [18-20]. The long range transport impacts of ground level  $O_3$  concentrations are best identified in the near ground boundary layer altitude [21].

The PSCF values for the  $ij^{\text{th}}$  cell were calculated by the following equation:

$$\text{PSCF}_{ij} = m_{ij}/n_{ij} \quad (3.3)$$



- Where,  $n_{ij}$  is defined as the total number of endpoints that occurs in the  $ij^{\text{th}}$  cell and  $m_{ij}$  is defined as the number of endpoints occurring in the  $ij^{\text{th}}$  cell which belongs to the trajectories corresponding to diel  $O_3$  events [13]. The PSCF values can be explained as

the conditional probability that  $O_3$  concentrations higher than the set criteria were in relation with the passage of air parcels through the  $ij^{\text{th}}$  cell throughout the transport to the receptor area. Higher PSCF value cells were related to the advent of air parcels at the receptor area which have ground level  $O_3$  concentrations higher than the set criteria. These cells specify the areas which have high concentrations of ground level  $O_3$  concentrations. A weighting function ( $w_{ij}$ ) was multiplied with the PSCF value to lower the effect of small total endpoint numbers by decreasing the effect of a small  $n_{ij}$  value and a weighted potential source contribution function (WPSCF) was obtained [17], shown in Eqs. (3.4) and (3.5) [22-24].

$$\text{WPSCF} = W_{ij} \times \text{PSCF} \quad (3.4)$$

$$W_{ij} = \left\{ \begin{array}{l} 1.00, 3n_{\text{mean}} < n_{ij} \\ 0.70, 1.5n_{\text{mean}} < n_{ij} = 3n_{\text{mean}} \\ 0.40, n_{\text{mean}} < n_{ij} = 1.5n_{\text{mean}} \\ 0.20, n_{ij} < n_{\text{mean}} \end{array} \right\} \quad (3.5)$$

### (C) Concentrated weighted trajectory (CWT)

CWT, which is a type of receptor model, is used to detect the local and regional source areas definitely influencing the receptor area. CWT calculations were done to recognize the sources of pollution effective in case of long term atmospheric measurements [17]. For CWT calculations, a weighted concentration is allocated in each grid cell by averaging the concentrations of the sample which have trajectories associated to them, crossing the grid cells and explained by the following equation:

$$C_{ij} = \frac{1}{\sum_{l=1}^M \tau_{ijl}} \sum_{l=1}^M C_l \tau_{ijl}, \quad (3.6)$$

Where  $C_{ij}$  is the average weighted concentration of  $O_3$  in the grid cell (i,j),  $l$  is the trajectory index,  $M$  is the total number of trajectories,  $C_l$  is the concentration perceived at the sampling site on advent of the trajectory  $l$ , and  $\tau_{ijl}$  is the consumed time of the trajectory  $l$  in the grid cell (i,j).

So, the concentration expected at the receptor site is represented by the weighted concentration obtained at each grid cell. Thus increase values of  $C_{ij}$  denotes that the air parcels advancing over the grid cell (i,j) would be, related with increased concentrations at the receptor area [25].

### **3.6: References**

1. Bhuyan, P., Deka, P., Prakash, A., Balachandran, S., & Hoque, R. R. Chemical characterization and source apportionment of aerosol over mid Brahmaputra Valley, India. *Environmental Pollution*, 234: 997-1010, 2018.
2. Census of India. [http://www.censusindia.gov.in/2011-prov-results/data\\_files/delhi/2\\_PDFC-Paper-1-major\\_trends\\_44-59.pdf](http://www.censusindia.gov.in/2011-prov-results/data_files/delhi/2_PDFC-Paper-1-major_trends_44-59.pdf), 2011.
3. Bhuyan, P., Barman, N., Bora, J., Daimari, R., Deka, P. and Hoque, R. R. Attributes of aerosol bound water soluble ions and carbon, and their relationships with AOD over the Brahmaputra Valley. *Atmospheric Environment*, 142:194- 209, 2016.
4. Ecotech Environmental monitoring, serinus 10 ozone analyzer, user manual, version 1.4, 2010.
5. Ecotech Environmental monitoring, serinus 40 oxides of Nitrogen analyzer, user manual, version 1.7, 2011.
6. Carslaw, D.C. Package “openair”. Tools for the Analysis of Air Pollution Data. Available from. [http:// david carsl aw. github. io/ opena ir/](http://davidcarslaw.github.io/openair/), Accessed date: February, 2018.
7. Carslaw, D. C., & Ropkins, K. Openair—An R package for air quality data analysis. *Environmental Modelling & Software*, 27:52–61, 2012.
8. Laskar, S. I., JASWAL, K., Bhatnagar, M. K., & Rathore, L. S. India meteorological department. *Proceedings of the Indian National Science Academy*, 82(3):1021-1037, 2016.

9. Vardoulakis S, Kassomenos P. Sources and factors affecting PM10 levels in two European cities: implications for local air quality management. *Atmospheric Environment*, 42: 3949–63, 2008.
10. Hatzianastassiou N, Katsoulis BD, Antakis B. Extreme nitrogen oxide and ozone concentrations in Athens atmosphere in relation to meteorological conditions. *Environmental Monitoring Assessment*, 128:447–64, 2007.
11. Bae MS, Schwab JJ, Chen WN, Lin CY, Rattigan OV, Demerjian KL. Identifying pollutant source directions using multiple analysis methods at a rural location in New York. *Atmospheric Environment*, 45:2531–40, 2011
12. Grivas G, Cheristanidis S, Chaloulakou A. Elemental and organic carbon in the urban environment of Athens. Seasonal and diurnal variations and estimates of secondary organic carbon. *Science of The Total Environment*, 414:535–45, 2012.
13. Dimitriou, K., & Kassomenos, P. Three year study of tropospheric ozone with back trajectories at a metropolitan and a medium scale urban area in Greece. *Science of The Total Environment*, 502: 493-501, 2015.
14. Lee JH, Hopke PK. Apportioning sources of PM2.5 in St. Louis, MO using speciation trends network data. *Atmospheric Environment*, 40:360–77, 2006.
15. Uria-Tellaetxe, I., & Carslaw, D.C. Conditional bivariate probability function for source identification. *Environmental modelling & software*, 59:1-9, 2014.
16. Draxler, R. R., and Hess, G. D. An overview of the HYSPLIT\_4 modelling system for trajectories, dispersion and deposition. *Australian Meteorological Magazine*, 47:295-308, 1998.
17. Wang, Y.Q., Zhang, X.Y., and Draxler, R.R. Trajstat: Gis-based software that uses various trajectory statistical analysis methods to identify potential sources from long-term air pollution measurement data. *Environmental Modelling and Software*, 24:938–939, 2009.
18. Dimitriou K, Kassomenos PA. Decomposing the profile of PMin two low polluted German cities — mapping of air mass residence time, focusing on potential long range transport impacts. *Environmental Pollution*, 190:91–100, 2014c.
19. Kavouras IG, Lianou M, Chalbot M-C, Vei IC, Kotronarou A, Hoek G, et al. Quantitative determination of regional contributions to fine and coarse particle mass in urban receptor sites. *Environmental Pollution*, 176:1–9, 2013.
20. Chalbot M-C, Lianou M, Vei I-C, Kotronarou A, Kavouras IG. Spatial attribution of sulfate and dust aerosol sources in an urban area using receptor modeling

- coupled with Lagrangian trajectories. *Atmospheric Pollution Research*, 4:346–53, 2013.
21. Makra L, Matyasovszky I, Guba Z, Karatzas K, Anttila P. Monitoring the long-range transport effects on urban PM10 levels using 3D clusters of backward trajectories. *Atmospheric Environment*, 45:2630–41, 2011.
  22. Kong X, He W, Qin N, He Q, Yang B, Ouyang H, et al. Comparison of transport pathways and potential sources of PM10 in two cities around a large Chinese lake using the modified trajectory analysis. *Atmospheric Environment*, 122:284–97, 2013.
  23. Karaca F, Anil I, Alagha O. Long-range potential source contributions of episodic aerosol events to PM10 profile of a megacity. *Atmospheric Environment*, 43:5713–22, 2009.
  24. Polissar AV, Hopke PK, Poirot RL. Atmospheric aerosol over Vermont: chemical composition and sources. *Environmental Science and Technology*, 35:4604–21, 2001.
  25. Chandra, S., Kulshrestha, M. J., & Singh, R. Temporal variation and concentration weighted trajectory analysis of lead in PM10 aerosols at a site in Central Delhi, India. *International Journal of Atmospheric Sciences*, 2014.